

## COMPARISON BASED BOTTOM-UP AND TOP-DOWN FILTERING MODEL OF THE HIPPOCAMPUS AND ITS ENVIRONMENT

ANDRÁS LÓRINCZ

**ABSTRACT.** Two rate code models – a reconstruction network model and a control model – of the hippocampal-entorhinal loop are merged. The hippocampal-entorhinal loop plays a double role in the unified model, it is part of a reconstruction network and a controller, too. This double role turns the bottom-up information flow into top-down control like signals. The role of bottom-up filtering is information maximization, noise filtering, temporal integration and prediction, whereas the role of top-down filtering is emphasizing, i.e., highlighting or ‘paving of the way’ as well as context based pattern completion. In the joined model, the control task is performed by cortical areas, whereas reconstruction networks can be found between cortical areas. While the controller is highly non-linear, the reconstruction network is an almost linear architecture, which is optimized for noise estimation and noise filtering. A conjecture of the reconstruction network model – that the long-term memory of the visual stream is the linear feedback connections between neocortical areas – is reinforced by the joined model. Falsifying predictions are presented; some of them have recent experimental support. Connections to attention and to awareness are made.

---

*Key words and phrases.* auto-associator, information processing, control, entorhinal cortex, reconstruction network.

Department of Information Systems  
Eötvös Loránd University  
Pázmány Péter sétány 1/C  
Budapest, Hungary H-1117  
email: lorincz@inf.elte.hu.

## 1. INTRODUCTION

Ever since the discovery of the central role of the hippocampus and its adjacent areas in memory formation [Sidman et al., 1968, Milner, 1972], numerous studies and models dealt with the properties and the possible functions of the hippocampus and its environment. The number of new experimental findings is increasing and highlight the complexity of the behavior of memory. Although views are strikingly different, they seem to have their own, experimentally supported merits. The interested reader is referred to the literature for excellent reviews on the hippocampus, e.g., [Squire, 1992], or [Hasselmo and McClelland, 1999] and [O’Reilly and Rudy, 1999]. The majority of the models have been developed to describe one part (mainly the CA3 field) of the hippocampus (see, e.g. [Levy, 1996, Káli and Dayan, 2000] and references therein). Some recent models have made attempts to develop an integrating model of the HC [Rolls, 1989, Hasselmo et al., 1996, Lisman, 1999, Eichenbaum, 2000, Hasselmo et al., 2002] and see also the collection of theoretical papers [Gluck, 1996]. It is known though, that hippocampus is deeply embedded in the neocortical information flow through the entorhinal cortex (EC). This fact explains the emergence of a few EC-HC models like [McClelland et al., 1995, Myers et al., 1995, Rolls, 2000]. Embedding is justified in most of them. For example, McClelland et al. ([McClelland et al., 1995]) emphasizes the necessity of a dual system for the seemingly contradictory tasks of learning specifications and allowing for generalization.

The computational model that we present here, has its origin in the old standing proposal that the hippocampus and/or its environment serve as a ‘comparator’ [Grastyán et al., 1959, Sokolov, 1963, Vinogradova, 1975]. There are more recent works along this subjects. Oftentimes models use somewhat different nomenclature, e.g., the focus is placed on match/mismatch detection [Ranck Jr., 1973, O’Keefe and Nadel, 1978, Grossberg, 1982]. Match/mismatch detection is closely related to familiarity/novelty detection, another direction of theoretical efforts to describe medial temporal lobe areas [Otto and Eichenbaum, 1992, Rolls et al., 1993, Wiebe and Saubli, 1999]. Note that precise distinction between orienting, salient and novel stimuli is not an easy matter [Rugg, 1995].

This work is about the merging two comparator based models: the control model of the entorhinal-hippocampal loop [Lőrincz, 1998] and the reconstruction network model of the same loop [Lőrincz and Buzsáki, 2000]. Both models have their own merits. For example, there is a large body of experimental data supporting the idea that attention shapes (influences, controls) perception. For excellent reviews, see, e.g., [Duncan, 1999, Posner and DiGirolamo, 2000, LaBerge, 2000] and references therein. The control model involves the comparator function, because – by construction – control concerns the difference between desired and actual parameters. On the other hand, the reconstruction network is also a comparator: it has a hidden layer, works as an auto-associator, and compares input to the auto-associated *reconstructed input*. It turns out that the reconstruction network is an appealing structure for experience based optimization of noise filtering [Lőrincz et al., 2002b]. We shall merge the two comparator structures and shall map the merged structure to the entorhinal-hippocampal loop and its environment. This

merging will enable us to make physiological predictions concerning persistent activities, delay properties, long-term memory and statistic versus one-shot learning.

There are two approaches, which should be mentioned, because both of them find their place in the present model. Gluck and Myers [Gluck and Myers, 1993] have designed a model to perform reconstruction *and* classification together for modeling some properties of the hippocampus. Rao and Ballard [Rao and Ballard, 1997, Rao, 1999, Rao and Ballard, 1999] have suggested an integrating model of the visual stream by exploring a Kalman-filter analogy to cope with the input and system uncertainties (treated as noise) and presented a hierarchy for error correction and prediction using top-down inference from higher levels. Kalman-filter is a kind of reconstruction or generative network, which uses an internal representation to generate expected inputs. The mapping of the proposed function onto the anatomical substrate has remained elusive. The Kalman-filter model, which is an approximation to our model, has been criticized because such recurrent loop structures are slow for feedforward processing found in neocortical areas [Koch and Poggio, 1999]. Our model resolves this problem.

Mathematical theorems and numerical studies concerning individual components and combinations of those have been presented elsewhere, or have been made available in the form of technical reports. For example, hierarchical reconstruction networks [Lőrincz et al., 2002b], the dynamics of the network as well as the order of learning in reconstruction networks [Lőrincz et al., 2002c], implicit memory phenomena, such as priming [Lőrincz et al., 2002c] and category formation in reconstruction networks [Kéri et al., 2002] are provided in the cited papers. Numerical studies concerning the control architecture can be found in [Szepesvári et al., 1997, Szepesvári and Lőrincz, 1997a, Szepesvári and Lőrincz, 1998]. Mathematical considerations as well as numerical studies of the control architecture embedded into the reinforcement learning framework have been thoroughly described in [Szita et al., 2003]. Connections to reinforcement learning, the key to fast, possibly one-shot memory encoding have been presented in [Kalmár et al., 1998, Szita et al., 2003] as well as in [Szita and Lőrincz, 2003]. The mathematical considerations have been complemented by some generalization concerning the control architecture in order to meet the requirements posed by the merging of the two architectures. This slight mathematical generalization can be found in the Appendix of a technical report [Lőrincz, 2003]. The novelty of the present work is in the merging of the two models and in the description how the two models can be merged. We shall find that stability properties of the controller are improved by the merging: The reconstruction network filters the input noise of the controller. (Considerations on noise sensitivity of the controller can be found in [Szepesvári and Lőrincz, 1997a].) Here, the model is described *by words* and *in figures*. The interested reader may wish to consult the cited works about the mathematical details.

In what follows, first, the terminology and the preliminaries are reviewed (Section 2). In Section 3, the merging of the control and reconstruction architectures into a single building block of a hierarchical structure is described. The closure of the hierarchy provides the view that the hippocampus plays a double role; it is part of a controller and contributes to a reconstruction network, too. Section 4 deals with the mapping of the control and reconstruction architectures to the entorhinal-hippocampal loop and its

environment. Physiological properties captured by the model as well as some falsifying predictions are listed and explained in this section. Conclusions are drawn in Section 5.

## 2. NOTATIONS AND PRELIMINARIES

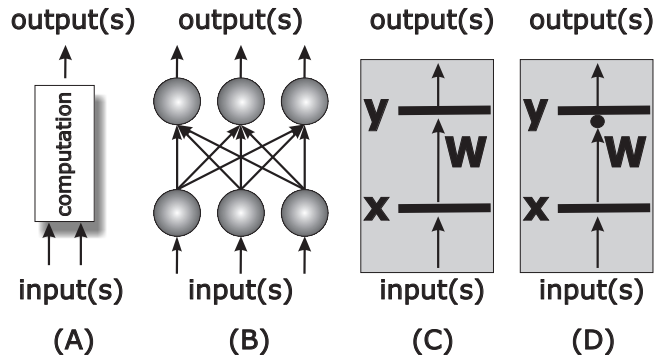


FIGURE 1. **Notations**

**A:** Control representation of input output systems. Computations are performed in the box.

**B:** Neural network representation of computations: inputs are received by input neurons and are (non-linearly) transformed by connections and the output neurons, which provide the outputs. An output neuron could be an input neuron of the next processing stage.

**C:** Linear neural transformation. Input:  $\mathbf{x}$ , transformation  $\mathbf{W}$ , output:  $\mathbf{y}$ ,  $\mathbf{y} = \mathbf{W}\mathbf{x}$ .

**D:** Non-linear neural transformation.  $\mathbf{y} = f(\mathbf{W}\mathbf{x})$ . Graphical form: arrow with a circle. More than one transformation may exist between layers. Recurrent network is a neural layer with a transformation that targets the same layer.

*Terminology in the context of neurobiology:*

Layer is encompassed by an area (e.g., typical neocortical areas are made of 6 layers), or it is a subfield, such as the CA3 and CA1 regions of the hippocampus. Transformations may correspond to (i) excitatory synapses connecting layers or targeting neurons of the same layer, such as the *recurrent collaterals* and the *associative connections* of the CA3 subfield of the hippocampus and the intra-layer excitatory connections of layers II and III of the neocortex or (ii) inhibitory synapses between layers or within layers, such as the rich interneural networks in the hippocampus.

Notations of the control field and notations of neuron networks differ. In control theory, input-output systems are considered. In graphical form, box denotes the system and arrows denote the system's input(s) and output(s). Processing occurs in the box (Fig. 1(A)). On the contrary, artificial neural networks consist of computational units, the putative analogs of real neurons. The units, also called neurons, receive (provide)

inputs (outputs) through the connection structure, and this internal functioning is drawn explicitly. Neurons execute simple computations, like summing up inputs, thresholding and alike. The main part of the neural network performs distributed computation using the connection structure performing (non-linear) filtering. This distributed filter system, which may connect all neurons, is called the connection system, weights, or synapses. In a neural network architecture, different neural layers are distinguished. Connections between these layers are explicitly drawn in most cases (Fig. 1(B)). Computations of neural networks between their inputs and outputs can be given in the following condensed form:

$$(1) \quad \mathbf{y} = f(\mathbf{W}\mathbf{x})$$

where input and output are denoted by  $\mathbf{x} \in \mathbb{R}^n$  and  $\mathbf{y} \in \mathbb{R}^m$ , respectively, linear transformation from  $\mathbb{R}^n$  to  $\mathbb{R}^m$  is represented by matrix  $\mathbf{W} \in \mathbb{R}^{m \times n}$ , the connections, and function  $f$  denotes a component-wise non-linearity. If this function is the identity function, then we have a linear network. Here, a simplified notation will be used: neural layers will be denoted by horizontal thick lines. Any particular set of connections between two layers will be represented by a single arrow. A feedforward linear network is depicted in Fig. 1(C). The graphical form of a network with component-wise non-linearity is shown in Fig. 1(D). Different transformations may exist between two layers. *Recurrent connections* (also called ‘recurrent collaterals’) target the same layer where they originate from. Equation 1 simplifies to the usual input-output mapping of a single neuron for  $m = 1$ .

## 2.1. Preliminaries.

**Controller.** Our control model is formulated in terms of state dependent directions pointing towards target positions. A mapping which renders direction (change of state, or change of state per unit time, i.e., velocity) to each state is called speed-field. A particular speed-field is given, for example, by the difference vectors between the target state and all other states. An important feature of speed-field is that motion is not specified in time. The control task is defined as moving according to the speed-field at each state. This control task is called speed-field tracking (SFT). For a review on SFT, see, e.g., [Hwang and Ahuja, 1992]. The control task of path (also called trajectory) tracking is different from SFT. This difference is illustrated in Fig. 2. One might say that SFT is less stringent and puts more emphasis on the global goal than on the tracking of a prescribed trajectory.

The dynamic equation of a system is a (possibly continuous) set of differential equations. This set of equations determines the change of state per unit time  $\dot{\mathbf{x}} \approx \frac{\Delta \mathbf{x}}{\Delta t}$  given the state of the plant (also called the system under control)  $\mathbf{x} \in \mathbb{R}^n$  and the external forces acting upon the system, including the control action  $\mathbf{u} \in \mathbb{R}^p$ . Let

$$(2) \quad \dot{\mathbf{x}} = \mathbf{f}(\mathbf{x}, \mathbf{u})$$

denote the dynamics of the system under control. This is what the system does.

Inverse dynamics works in the opposite way: given the state and (desired) change of state, inverse dynamics provides the control vector. The controller, in turn, maps state and speed to control action. Let  $\mathbf{v}(\mathbf{x}) \in \mathbb{R}^n$  denote the *desired* change of state (the desired

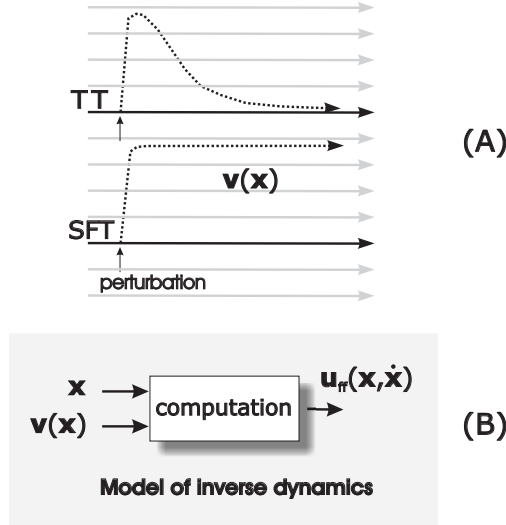


FIGURE 2. **Tracking and inverse dynamics)**

**A: TT:** Horizontal lines represent different nearby trajectories in 2 dimensions. Black line: initial trajectory. Dotted line: perturbed trajectory. Upon perturbations the system (the ‘plant’) should return to the original trajectory, which is also specified in time (not shown).

**SFT:** Horizontal lines represent a small homogeneous part of a speed-field  $\mathbf{v}(\mathbf{x})$  to be tracked embedded into a 2 dimensional space  $\mathbf{x}$ . Black line: initial speed trajectory. Dotted line: perturbed motion. Upon perturbation, the plant adjusts its speed to the prescribed speed in its actual neighborhood.

**B:** Inverse dynamics produces a control vector for a given pair of state and the belonging desired speed.

momentum). Assume that we have an approximate feedforward model of the inverse dynamics:

$$(3) \quad \mathbf{u}_{ff} = \mathbf{u}_{ff}(\mathbf{x}, \mathbf{v}(\mathbf{x}))$$

$$(4) \quad = \mathbf{A}(\mathbf{x})\mathbf{v}(\mathbf{x}) + \mathbf{b}(\mathbf{x})$$

where  $\mathbf{A}(\mathbf{x}) \in \mathbb{R}^{n \times n}$ ,  $\mathbf{b}(\mathbf{x}) \in \mathbb{R}^n$ . Equation 3 represents an input-output system receiving the state and the desired momentum, which is denoted by  $\mathbf{v}(\mathbf{x})$  and providing output (the control vector  $\mathbf{u}_{ff} : \mathbb{R}^{n \times n} \rightarrow \mathbb{R}^p$ ). This control vector could be used directly to influence the plant and it is called *feedforward controller*. If the inverse dynamics is perfect then using this control vector directly, that is inserting this control vector into the dynamic equation  $\dot{\mathbf{x}} = \mathbf{f}(\mathbf{x}, \mathbf{u})$ , the desired change of state is achieved: The perfect feedforward control vector  $\mathbf{u}_{ff}^*$  makes the plant to produce momentum  $\mathbf{v}(\mathbf{x})$ :

$$(5) \quad \mathbf{v}(\mathbf{x}) = \mathbf{f}(\mathbf{x}, \mathbf{u}_{ff}^*(\mathbf{x}, \mathbf{v}(\mathbf{x})))$$

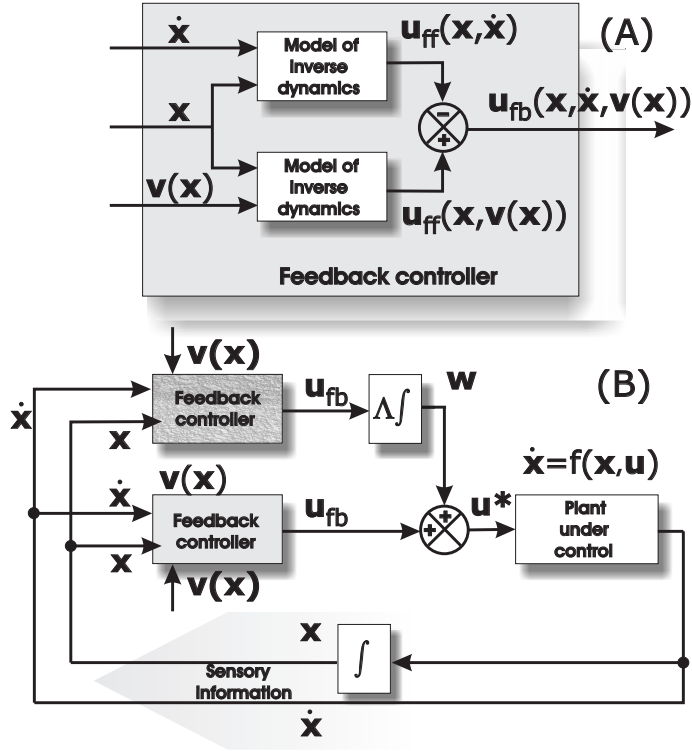


FIGURE 3. Robust controller for speed-field tracking tasks

**A:** The model of the inverse dynamics is inputted by the actual state  $\mathbf{x}$  and the desired momentum (or desired speed vector)  $\mathbf{v}(\mathbf{x})$ . The output of the model is the *feedforward* control vector  $\mathbf{u}_{ff} = \mathbf{u}_{ff}(\mathbf{x}, \mathbf{v}(\mathbf{x}))$ . The feedforward control vector may need corrections. The *feedback* control vector is the difference between the feedforward control vector and the *experienced control vector*  $\mathbf{u}_{ff}(\mathbf{x}, \dot{\mathbf{x}})$ :  $\mathbf{u}_{fb} = \mathbf{u}_{ff}(\mathbf{x}, \mathbf{v}(\mathbf{x})) - \mathbf{u}_{ff}(\mathbf{x}, \dot{\mathbf{x}})$ .

**B:** The static and dynamic state (SDS) feedback controller. The output of the feedback controller is (i) applied directly and (ii) it is integrated by time multiplied by the gain factor and the result is added to form the almost correct control vector  $\mathbf{u}^*$ . *Differing texture* of the two feedback controllers denotes that computations in these input-output devices can differ as long as certain mathematical conditions concerning the sign of the components of the control vectors are met.

If the feedforward control vector is imprecise then error (a difference between the desired momentum and the experienced momentum)  $\mathbf{e}_c = \mathbf{v}(\mathbf{x}) - \dot{\mathbf{x}}$  appears. To correct this error, the (same or another) model of the inverse dynamics can be used. The error correcting controller is called *feedback controller* [Szepesvári et al., 1997]: The output of the feedback controller  $\mathbf{u}_{fb}$

$$(6) \quad \mathbf{u}_{fb} = \mathbf{u}_{ff}(\mathbf{x}, \mathbf{v}(\mathbf{x})) - \mathbf{u}_{ff}(\mathbf{x}, \dot{\mathbf{x}})$$

can be temporally integrated

$$(7) \quad \mathbf{w}(t) = \int_{-\infty}^t \dot{\mathbf{w}} dt = \int_{-\infty}^t \Lambda \mathbf{u}_{fb} dt$$

and the two terms, together:

$$(8) \quad \mathbf{u}^* = \mathbf{u}_{fb} + \mathbf{w}$$

provide an globally stable and almost perfect controller [Szepesvári and Lőrincz, 1997a, Lőrincz, 2003]. This scheme is depicted in Fig. 3. Note that Eq. 4 allows one to write  $\mathbf{u}_{fb}$  as

$$(9) \quad \mathbf{u}_{fb} = \mathbf{A}(\mathbf{x})(\mathbf{v}(\mathbf{x}) - \dot{\mathbf{x}})$$

The controller allows for temporal changes of the non-linear terms  $\mathbf{A}(\mathbf{x})$  and  $\mathbf{b}(\mathbf{x})$ , a rare property in the control literature. The condition of this property make the working of the architecture strongly non-linear [Lőrincz et al., 2001] and will be discussed later. Also, the two feedback controllers of Fig. 3(B) can differ [Lőrincz, 2003].

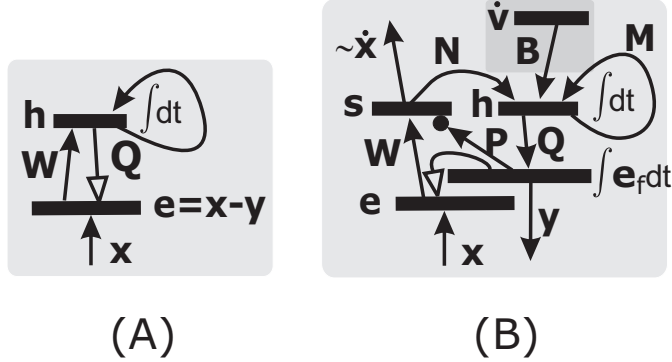
$$(10) \quad \dot{\mathbf{w}} = \Lambda \mathbf{A}(\mathbf{x})(\mathbf{v}(\mathbf{x}) - \dot{\mathbf{x}})$$

$$(11) \quad \mathbf{u}^* = \hat{\mathbf{A}}(\mathbf{x})(\mathbf{v}(\mathbf{x}) - \dot{\mathbf{x}}) + \mathbf{w}$$

where  $\mathbf{A}$  can be different from  $\hat{\mathbf{A}}$ . Both controllers operate by *comparing* ‘desired’ and ‘experienced’ quantities. Under certain conditions, global stability is reached by the two controllers. The proof relies on an extension to Ljapunov’s second method [Szepesvári et al., 1997, Szepesvári and Lőrincz, 1997a, Szepesvári and Lőrincz, 1997b, Lőrincz, 2003]. The controller architecture of Fig. 3 is called the static and dynamic state feedback controller, or SDS controller, for short.

## Reconstruction network.

**Basic reconstruction network.** The basic reconstruction network (Fig. 4(A)) has two layers: the reconstruction error layer and the hidden layer. The reconstruction error computes the difference ( $\mathbf{e} \in \mathbb{R}^r$ ) between input ( $\mathbf{x} \in \mathbb{R}^r$ ) and reconstructed input ( $\mathbf{y} \in \mathbb{R}^r$ ):  $\mathbf{e} = \mathbf{x} - \mathbf{y}$ . Reconstructed input  $\mathbf{y}$  is produced by the hidden (internal) representation  $\mathbf{h} \in \mathbb{R}^s$  via top-down transformation  $\mathbf{Q}$  where  $\mathbf{Q} \in \mathbb{R}^{r \times s}$  and  $r \leq s$  or  $r > s$  are both possible at the expense of some mild non-linearities (see, e.g., [Olshausen and Field, 1997] and references therein). The hidden representation is corrected by the bottom-up transformed form of the reconstruction error  $\mathbf{e}$  that is by  $\mathbf{W}\mathbf{e}$  (where  $\mathbf{W} \in \mathbb{R}^{s \times r}$ ). The process of correction means that the previous value of the hidden representation is to be maintained and the correcting amount needs to be added. In turn, the hidden representation has a self-excitatory connection set, which maintains the activities. Correction occurs in time and this (continuous or discrete) temporal collection of correcting terms is denoted by  $\int dt$ . For sustained input  $\mathbf{x}$  the iteration will stop when  $\mathbf{Q}\mathbf{h} = \mathbf{x}$  or when the bottom-up transformed values of  $\mathbf{Q}\mathbf{h}$  and  $\mathbf{x}$  are equal:  $\mathbf{W}\mathbf{Q}\mathbf{h} = \mathbf{W}\mathbf{x}$ . In turn, for each input, the hidden representation is determined by top-down transformation  $\mathbf{Q}$ . The bottom-up transformation can restrict the range of the reconstruction. For example, if  $\mathbf{W}$  projects to a subspace then reconstruction can be executed only within that subspace.

FIGURE 4. **Reconstruction networks**

**A:** Simplest reconstruction network.  $x$  and  $y$ : input and reconstructed input, respectively,  $W$  and  $Q$ : bottom-up (BU) and top-down (TD) transformations, respectively.  $\int dt$ : summation in (or integration by) time.

**B:** Reconstruction network capable of noise filtering and pattern completion.  $s$ : BU processed reconstruction error with maximized information,  $h$ : activity vector of the hidden (model) layer,  $N$ : transformation from BU processed reconstruction error layer to the model layer.  $P$ : linear BU transformation followed by sparsifying thresholding. Thresholding gates components that deliver noise, but no information. For a perfectly tuned network,  $P = W$ , and either  $QNW = I$  ( $s \leq r$ ) or  $NWQ = I$  ( $r \leq s$ ).  $M$ : recurrent collateral system for temporal integration and pattern completion. Dark gray inset:  $B$  and  $\dot{v}$  are tools of control. The controller provides the temporal derivative of the control vector  $Bv$ , where  $v$  is the desired momentum of the controller. The derivative  $B\dot{v}$  is integrated at the internal representation.

For  $s \leq r$ , we call the network perfectly tuned if  $W = (Q^T Q)^{-1} Q^T$ , i.e., if  $WQ = I$  ( $I \in \mathbb{R}^{s \times s}$ ). In this case, activities of the hidden layer become perfect after a single bottom-up processing step and the network works alike to feedforward nets.

**Reconstruction network plus.** The simple network of Fig. 4(A) can be extended to support noise filtering. To this purpose, the reconstructed input vector  $y$  is represented separately. Input vector  $x$  is compared to the reconstructed input  $y$  in the error layer:  $e = x - y$ . The error is transformed by the bottom-up (BU) transformation matrix  $W$  and forms the BU transformed error  $s$ . BU transformation maximizes BU information transfer in order to facilitate reconstruction. BU transformed error is passed to the internal representation layer through transformation matrix  $N$  (the role of this transformation shall be discussed later) and is added to the internal representation  $h$  of the ‘hidden’ (or model, or internal representation) layer. The activity of the hidden layer is maintained by diagonal elements of recurrent matrix  $M$ , which – beyond temporal integration – can support category formation [Kéri et al., 2002] as well as temporal prediction [Rao and Ballard, 1997] via its off-diagonal elements.

The network of Fig. 4(B) works as follows. Off-diagonal elements of recurrent matrix  $\mathbf{M}$  of the hidden layer perform pattern completion [Lörincz et al., 2002b] and temporal prediction [Rao and Ballard, 1997]. The newly introduced layer denoted by  $\mathbf{s}$  ( $\mathbf{s} \in \mathbb{R}^r$ ) will be called the ICA layer. This ICA layer plays a role in noise filtering. There are two different sets of afferents to the ICA layer: one is carrying the BU transformed error, whereas the other carries information about the reconstructed input  $\mathbf{y}$  via bottom-up transformation  $\mathbf{P}$ , followed by a non-linearity that removes noise via thresholding. Thresholding is alike to wavelet denoising [Mallat, 1998], with the exception that the filters are not necessarily wavelets but are optimized for the input database experienced by the network. Optimization makes use of independent component analysis (ICA) [Jutten and Herault, 1991, Comon, 1994, Laheld and Cardoso, 1994, Bell and Sejnowski, 1995, Amari et al., 1996, Karhunen et al., 1997, Amari, 1998]. ICA makes the assumption that input is generated by statistically independent sources

$$(12) \quad \mathbf{x} = \mathbf{C}\mathbf{r} + \nu$$

$$(13) \quad P(r_1, \dots, r_r) = \prod_{k=1}^r P(r_k)$$

where  $\nu \in \mathbb{R}^r$  denotes additive Gaussian noise,  $\mathbf{r} \in \mathbb{R}^r$  denote the original sources and  $\mathbf{C} \in \mathbb{R}^{r \times r}$  is called the mixing matrix. The ICA algorithm intends to reproduce the original sources and minimizes mutual information between ICA transformed components. The multiplication of vector  $\mathbf{r}$  by matrix  $\mathbf{C}$ , makes the identification of matrix  $\mathbf{C}$  ill posed: The problem becomes well posed, by constraining the variances of the searched components. For example, variances can be constrained to one. In this case, minimization of mutual information is equivalent to maximizing the sum of the *negentropies* (the non-Gaussian character) of uncorrelated estimates [Hyvärinen et al., 1999]. This feature enables the local estimation and local thresholding of noise components [Hyvärinen et al., 1999, Hyvärinen, 1999], where locality means that noise of each component of the ICA layer can be thresholded independently of the value of other ICA components. The method is called sparse code shrinkage (SCS) and the process is referred to as sparsification.

Thus,  $\mathbf{s}$  is the ICA transformed and sparsified reconstruction error. Note however, that sparsification concerns the components of the BU transformed reconstructed input: high amplitude components of  $\mathbf{P}\mathbf{y}$  (BU transformed reconstructed input) open the gates of components of the ICA layer and ICA transformed reconstruction error can pass these open gates to correct the internal representation. Low amplitude components of  $\mathbf{P}$  transformed reconstructed input can not open the gates and corrections of these components are rejected, unless the correction themselves are large enough to overcome the sparsification process.

Apart from sparsification, the reconstruction network is a linear network. In what follows, we shall denote this property by the notations sign ‘ $\sim$ ’.  $A \sim B$  means that for a well tuned system and up to a scaling constant (or scaling matrix) quantity  $A$  is approximately equal to quantity  $B$ .

For a well tuned network and if matrix  $\mathbf{M}$  performs temporal integration (i.e., if matrix  $\mathbf{M}$  does not perform temporal prediction),  $\mathbf{s} \sim \dot{\mathbf{x}}$  by construction. If matrix  $\mathbf{M}$  performs temporal prediction and the network is perfectly tuned, then  $\mathbf{s} \sim \ddot{\mathbf{x}}$ . These quantities could be processed and represented at higher layers. For the sake of simplicity of considerations, assume that matrix  $\mathbf{M}$  performs temporal integration and nothing else. Then we can approximate the output of layer  $\mathbf{s}$  as a noise filtered linearly transformed (i.e., filtered and scaled) form of  $\dot{\mathbf{x}}$ .<sup>1</sup> We shall further simplify the notation. The output of the ICA layer will be denoted by  $\sim \dot{\mathbf{x}}$ , where  $\sim \dot{\mathbf{x}}$  means ‘the scaled version’ of  $\dot{\mathbf{x}}$ . In a similar vein, internal representation  $\mathbf{h} \sim \mathbf{y}$ . Also, we shall use the notation  $\mathbf{y} \sim \mathbf{x}$ , although the former is the noise filtered version of the latter.

Note that considerable reconstruction error can build up, e.g., by top-down influence. Considering longer temporal scales, then – by construction –  $\mathbf{y}$  is equal to the temporal integral of the noise filtered reconstruction error:  $\mathbf{y} = \int \mathbf{e}_f dt$  where  $\mathbf{e}_f$  denotes the noise filtered reconstruction error. This feature will be exploited later.

### 3. THE JOINED MODEL

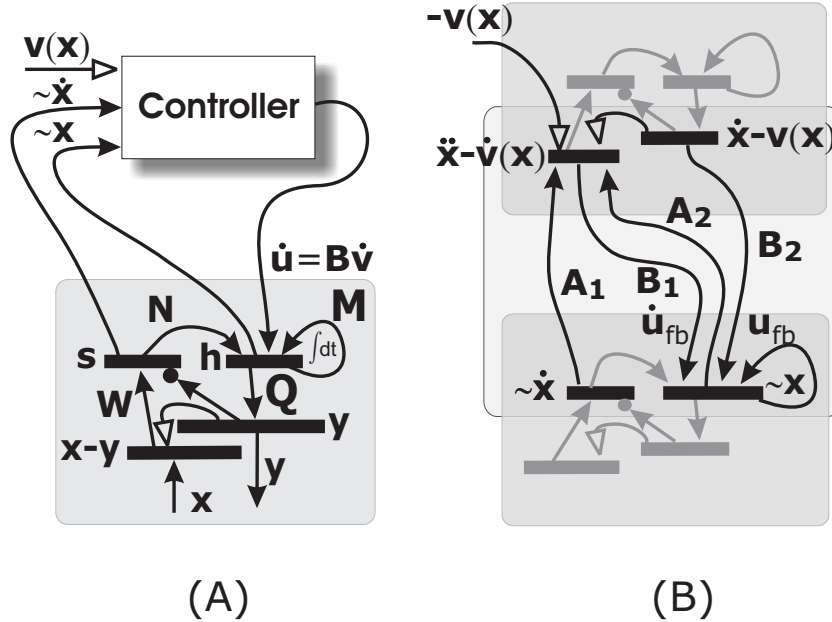
**3.1. Controlled reconstruction network.** The reconstruction network can be controlled (Fig. 5(B)). Control adds extra contribution to the hidden layer, namely  $\mathbf{B}\dot{\mathbf{v}}$ . The ‘dot’ on  $\mathbf{v}$  is the consequence of adding the contribution to the internal representation where temporal integration occurs. In turn, the action of the controller is equal to the temporally integrated value of the extra contribution, that is  $\mathbf{B}\mathbf{v}$ .

To achieve approximately perfect controlling, we shall make use of the SDS controller. The controller is made of another (‘higher’) reconstruction network, which receives input from the network under controlled (the ‘lower’ network). This input is equal to the output of the ICA layer of the lower network. Control works by subtracting the desired speed from the input of the higher network. That makes the input to the network equal to  $\dot{\mathbf{x}} - \mathbf{v}(\mathbf{x})$ .<sup>2</sup> By construction, (i) the input is noise filtered and reconstructed at the reconstructed input of the network and (ii) apart from the noise content, the error layer approximates the temporal derivative of the reconstructed input (Fig. 5(B)). These two differences undergo linear transformation and enter the internal representation layer of the lower network, where – by construction – they add up and undergo temporal integration. This is exactly what is needed for the SDS controller. Moreover, noise filtering of the reconstructed input is of particular importance, because noise entering temporal integration seems to be the weakest point of the controller [Szepesvári and Lőrincz, 1997a].

Learning to control in the SDS scheme is relatively simple. Roughly speaking, learning is sufficient if the signs of the components of the control vector and the domains where these components should not change sign have been determined. This is why the negative negative sign of  $\dot{\mathbf{x}} - \mathbf{v}(\mathbf{x})$  (instead of  $\mathbf{v}(\mathbf{x}) - \dot{\mathbf{x}}$ ) does not count: signs of components of matrix  $\mathbf{B}$  need to be determined by learning. SDS warrants that if the signs of the control

<sup>1</sup>Extension to spatio-temporal pattern completion is straightforward. Redefining the state as the concatenation of  $\mathbf{x}$  and  $\dot{\mathbf{x}}$  and speed as the concatenation of  $\dot{\mathbf{x}}$  and  $\ddot{\mathbf{x}}$  gives rise to the same formalism that we are using here [Szepesvári and Lőrincz, 1997a].

<sup>2</sup>Note the negative sign of this difference that we shall discuss in the next paragraph

FIGURE 5. **Controlled networks**

*Notation:*  $\sim \mathbf{z}$ : scales (approximately) linearly with  $\mathbf{z}$ .

**A:** Controller receives the state ( $\sim \mathbf{x}$ ) and the speed ( $\sim \dot{\mathbf{x}}$ ) from the reconstruction network under control as well as the desired speed ( $\mathbf{v}(\mathbf{x})$ ) from somewhere else and forms the difference between them.

**B:** Reconstruction network acting as a controller.  $\mathbf{A}_1$  and  $\mathbf{A}_2$  carries information about the state and the speed of the network under control, respectively. Difference between speed and desired speed is the input to the network. The noise filtered and reconstructed value of this difference appears at the reconstructed input. By construction, the reconstruction error layer holds – the approximate – temporal derivative of the reconstructed input. These differences are turned into feedback control vector  $\mathbf{u}_{fb}$  and its temporal derivative  $\dot{\mathbf{u}}_{fb}$  by means of transformations  $\mathbf{B}_2$  and  $\mathbf{B}_1$ , respectively. The outputs of these transformation are temporally integrated at the internal representation of the lower network to form the components of the SDS controller. They add up here and provide almost perfect and stable control.

components are proper, then control will be globally stable and approximately perfect. Mathematical details of *sign-properness* can be found elsewhere [Szepesvári et al., 1997, Szepesvári and Lőrincz, 1997a, Lőrincz, 2003]. Numerical demonstrations using coarsely tuned but sign-proper controllers have been provided in [Lőrincz et al., 2001].

The hierarchy is highly non-linear because of several reasons. The higher the reconstruction network in the hierarchy, the higher the order of the dynamic properties of the environment that are learned and represented by it. Also, the condition of robust control

concerns the shattering of the space to sign-proper domains and the dynamic contribution of the controller can be highly non-linear within sign-proper domains. Switching between domain is highly non-linear, too. Lastly, sparsification is another source of non-linear processing.

Another note concerns the result of controlling. The SDS controller warrants that the desired quantity is closely approximated under the condition that the system is controllable. Until this point control concerned a lower reconstruction network, which may receive input from the environment (Fig. 5(B)). Conditions of the SDS controller are not fulfilled unless control action also concerns this input, or if this input is zero. In the former case, control of the environment needs to be included into the architecture. The latter case corresponds to the absence of external inputs, such as pattern completion or dreaming.

The perfectly tuned architecture behaves as a bottom-up feedforward network, which is biased by top-down influence. Consider the lower reconstruction network of Fig. 5(B). The bias will modify the internal representation of the lower reconstruction network, which may or may not fit the input from the environment. If it fits, then any reconstruction error disappears quickly. In case if it does not fit, large reconstruction error at the reconstruction error layer may build up, but only a small portion of this error can pass the sparsification process at the ICA layer. This is because sparsification is ruled by the internal representation generated reconstructed input. That is, information that matches the *context* of the higher reconstruction network will be able to pass sparsification, whereas other information will be *filtered out*, or attenuated by the bottom-up sparsification process. In turn, top-down influence ‘paves the way’ of some of the components. The process of filtering out certain components of information and paving the way of the others can be seen as *attention is paid* to the latter components.

**3.2. Closing the loops of the hierarchy.** The top of the hierarchy has a special role. At the top, the sensory bottom-up information flow should be turned into context like top-down information, which can enforce, shape, or influence (say, control) lower representations. This reversal of the direction of information flow becomes possible if the reconstruction error feeds the internal representation of a *lower* reconstruction network. In this case, we shall have a network with a reconstruction error layer and an internal representation, which when put together, make up a reconstruction network. On the other hand, we have also a controller, because error at a higher level guides the internal representation of a lower level. The idea is illustrated in Fig. 6(A). The figure uses the same gray coding that Fig. 5: dark and light gray areas correspond to reconstruction and control networks, respectively. There are two dark and two light areas. All of the components are depicted, but some of them are denoted by lighter dashed lines. These connectivity structures and neural layers are missing at the top. Notation corresponds to the cortical layers. Layers  $\mathbf{x}$ ,  $\mathbf{y}$ ,  $\mathbf{s}$ , and  $\mathbf{h}$  represent superficial layers II, III, granular layer IV, and deep layers V-VI, respectively. The highest layer is denoted by HC, the short for hippocampus. The upper control layer is denoted by EC, the short for the entorhinal cortex.

The following differences are to be noted. First, there is no top-down connection from EC layers II and III to EC the deep layers. In turn, these layers can not exert control action onto the corresponding internal representation. Instead, the HC is in the

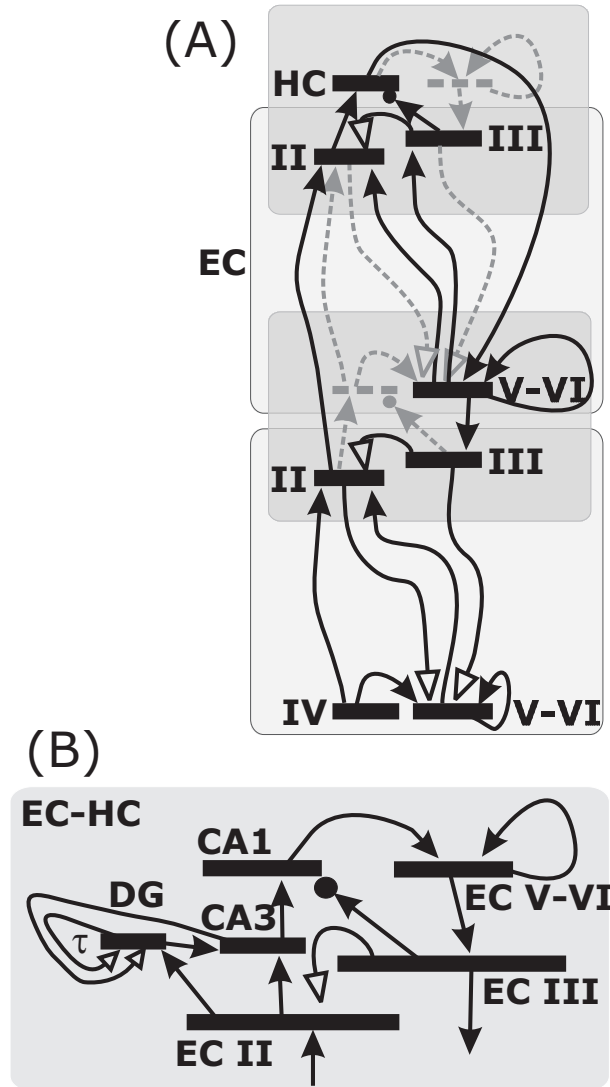


FIGURE 6. **The top of the hierarchy**

**A:** HC: hippocampus. II-III: superficial layers. IV: granular layer. V-VI: deep layers. The top turns information flow from bottom-up direction to top-down direction: HC acts on the internal representation of a lower reconstruction network. HC together with the layers encompassed by the grey box indexed by EC, i.e., the entorhinal cortex, which has no granular layer, form a reconstruction network.

**B:** Mapping of the top to the EC-HC loop. ICA is made in two steps: (i) whitening (CA3 subfield of HC) and (ii) separation (CA1 subfield of HC). Blind source deconvolution, the putative role of the dentate gyrus, removes temporal correlations. Reconstruction error is computed at EC layer II. Reconstructed input: EC layer III. Internal (hidden) representation: EC layers V and VI. Temporal integration (persistent activities) and possibly pattern completion is the putative role of the recurrent collaterals of EC layers V and VI. EC afferents of area CA1: denoising.

position to exert control action: it receives the reconstruction error from the lower layer and acts upon the hidden representation of that reconstruction network. On the other hand, consider the connectivity of the deep layers of the EC, the superficial layers of the EC and the HC. These structures, together, form a reconstruction network. It can be easily verified by shifting the deep layers of the EC next to the HC in Fig. 6(A). In turn, the HC and its environment has a double role, it is a control network and a reconstruction network. The control network acts upon a lower internal representation that reverses the bottom-up flow of sensory information into top-down control making use of the context of higher reconstruction networks. Using the concepts of the controller hierarchy, higher order dynamical information corrects lower order approximations.

Note that information flow from the lowest layers ( $\mathbf{s}$  and  $\mathbf{h}$ ) passes through the ladder of two reconstruction error layers (superficial layer II). This feature can not be explained within the framework of the model. It allows us to pin-point to the limitations of our modelling efforts. The functional model can not explain the recurrent collaterals of the superficial layers, a prominent structure of neocortical regions. This connectivity is thought as the extension of the associative cortices (see, e.g., [Diamond, 1979] and references therein). Our model suggests that two of such layers can be seen as a single but larger layer, which is in agreement with the functionality suggested by Diamond.

Detailed description of the HC has been provided elsewhere [Lőrincz and Buzsáki, 2000, Lőrincz et al., 2002b] and will be reviewed in the next section.

#### 4. DISCUSSION

Our first note concerns Adaptive Resonance Theory (ART) pioneered by Grossberg and colleagues [Grossberg, 1980, Carpenter and Grossberg, 1987, Raizada and Grossberg, 2003]. ART proposes that sensory processing is two-folded: It is made of bottom-up filtering as well as of top-down template matching. The underlying mechanism of ART – namely, the resonant circuitry – differs from the two-folded comparator function embodied by our architecture. Mapping to the neurobiological substrate [Grossberg and Carpenter, 1993, Raizada and Grossberg, 2003] is, in turn, different from ours that we shall present below.

Our modelling efforts have certain particular properties: We have started from functional hypothesis about the importance of control and noise filtering and have introduced a hierarchical system, which should be capable to do both. At each step, mathematical tools were used to restrict our freedom. Possible solutions, which were untractable from the point of view of stability and noise filtering, or, alternatively, which could not be mapped to the anatomical structure, or did not fit known physiological properties and known results of computational neuroscience were dropped [Lőrincz et al., 2000]. We call this function based, structure constrained and mathematics supported effort, Ockham's modelling [Lőrincz et al., 2001, Lőrincz et al., 2002a]. ART does the same. Our comparator model is different, because it starts from control principles control principles and assumes the universality of the comparator hypothesis. For a control network, comparison between desired and experienced quantities seems reasonable.

The model offers falsifying predictions; i.e., predictions which could constrain or defeat the model. These predictions will be listed below. First, we shall provide the mapping to the substrate, a most crucial constraint for us. The mapping of the reconstruction network has been elaborated before [Lőrincz et al., 2002b]. It is reviewed here for the sake of completeness.

**4.1. Matching the anatomy.** The neocortex is made of six sub-layers (Fig. 7). The figure depicts the most prominent connections between these sub-layers [Lund, 1988]. Input typically arrives at layer IV. Layer IV neurons send messages to layer II and layer III (not shown). Furthermore, layer IV neurons send messages also to layer VI. Superficial neurons provide output down to layer V and VI. There are connections between neurons of layer V and layer VI. Neurons of layer II and III are also strongly connected. Layer V provide feedback to layers II and III. The main output to higher cortical layers emerges from layers II and III. The main feedback to lower layers is provided by layer V. (For a review see, e.g., [Callaway, 2000].)

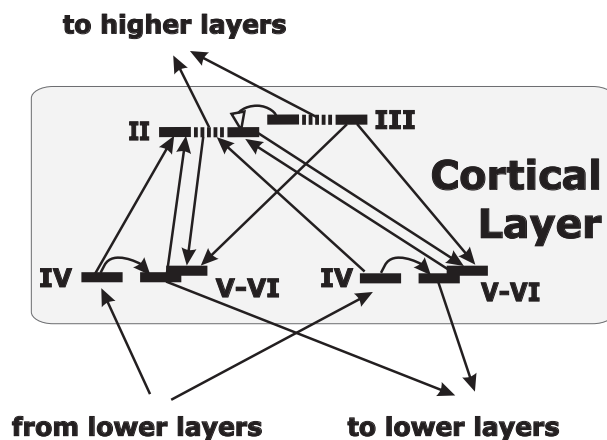


FIGURE 7. Neocortical layer

The theoretical model and the anatomical structure can be matched by assuming that reconstruction networks are laid *between* neocortical layers as it was denoted by the dark gray areas in Fig. 6(A) [Lőrincz et al., 2002b]. According to this figure, superficial layers of the lower cortical layer *and* deep layers of the higher cortical layer form *one* functional unit, the reconstruction network.

The novel anatomical suggestion of this paper is the mapping of a robust controller to the cortical layers (denoted by light gray boxes of Fig. 6(A)). The reconstruction error and the noise filtered temporal integral of this error, that is the reconstructed input exerts control action on lower reconstruction networks that corresponds to the information sent from superficial layers to deep layers. Experienced quantities correspond to the information propagating into the other direction, i.e., experienced quantities are sent to superficial layers by layers IV and V.

Mapping of the top to the EC-HC loop is shown in Fig 6(B). Independent component analysis is executed in two steps: (i) whitening (CA3 subfield of HC) and (ii) separation (CA1 subfield of HC). Reconstruction error and reconstructed input are computed in EC layer II and EC layer III, respectively. Internal (hidden) representation is encompassed by EC layers V and VI. These deep layers perform the pattern completion task. The EC afferents of the CA1 subfield can release the gates of the CA1 outputs and denoised signals can pass. The recurrent collaterals of the CA3 subfield replay learned sequences. Blind source deconvolution (BSD) is the putative role of the dentate gyrus. BSD removes temporal correlations cumulated by temporal integration of not-yet tuned lower reconstruction networks. BSD is necessary for proper ICA analysis. However, the number of neurons of a BSD structure can be very large. It is assumed that this computation can be afforded only at the top of the hierarchy. In turn, the dentate gyrus plays a unique role in our model. The assumption gains further support from top-down controlling: control can accelerate reconstruction [Lőrincz, 1998]. In turn, BSD at lower networks may not be necessary. This point deserves further investigations. More details can be found elsewhere [Lőrincz and Buzsáki, 2000].

**4.2. Predictions of the model.** Lőrincz and colleagues have shown previously that some memory effects, such as repetition suppression and priming [Lőrincz et al., 2002c] as well as the particular properties found for Alzheimer patients in a classic prototype learning paradigm (see, e.g., [Knowlton, 1999] and references therein about ‘9 dot’ experiments) can be explained by the reconstruction network model [Kéri et al., 2002].

A crucial prediction of our model is that temporal convolutions should be removed before ICA occurs. Given that ICA is the putative role of the CA3 and CA1 subfields, only the dentate gyrus can be responsible for this task. In turn, long and tunable delay lines should exist in the dentate gyrus. This prediction has been reinforced recently [Henze et al., 2002].

Another falsifying prediction of the model concerns the internal representation layer, which has to maintain its own activities in order to enable additive corrections and temporal integration. Persistent activities in the deep layers but not in the superficial layers of the EC have been found experimentally [Egorov et al., 2002].

An intriguing and falsifying prediction of the joined model, alike to its previous versions [Lőrincz and Buzsáki, 2000], is that top-down connections of reconstruction networks can be interpreted as long-term memories (LTMs), because these connections are responsible for the relaxed activities of the hidden layers. Given our mapping, the LTM corresponds to feedback connections between neocortical areas. These connections are generally more numerous than the feedforward connections between the same areas but the activity flow along these connections is relatively low and suggests a weak functional role (see, e.g., [Callaway, 2000] and references therein). This apparent discrepancy may be resolved by noting that different interpretations may coexist in the brain as it has been made evident in the animal experiments on binocular rivalry (see, e.g., [Leopold and Logothetis, 1999] and references therein) and in experiments with several possible visual interpretations (see, e.g., [Leopold, 2003, Parker and Krug, 2003] and the cited references). If reconstruction concerns a single interpretation then feedback activity flow should be *small*. This possibility

can not be excluded because of the following reasons. There are evidences that activities in V4 (responsible for conscious detection of colors) and V5 (responsible for conscious detection of fast motion) in the monkey are uncorrelated. According to the arguments put forth by Zeki [Zeki, 2003], uncorrelated activities indicate that conscious experiences propagate downwards along parallel channels. Moreover, the conscious binding of the result of the individual conscious experiences seems to be delayed [Bartels and Zeki, 2002]. In turn, it is possible that only one interpretation is communicated downwards at a time. Another point concerns the suggested function, that the internal representation is under top-down control. This controlled representation will then propagate downwards to form the reconstructed input and also directly to real control networks [Diamond, 1979]. Given the long delays of processing, a well tuned control system should not interact oftentimes. In turn, the assumed function involves relatively sparse information flow.

It is important to note that in the original *control* model of the EC-HC loop [Lőrincz, 1998] the dentate gyrus was suggested as the source of temporal integration. Only the making of the reconstruction network model [Lőrincz and Buzsáki, 2000, Chrobak et al., 2000] revealed that temporal integration has to be executed at the hidden layer and not at the dentate gyrus, whereas temporal convolutions produced by temporal integrations accomplished in lower networks can be removed by means of the BSD algorithm at the dentate gyrus.

According to recent measurements, awareness and attention needs to be distinguished (for an excellent review, see [Lamme, 2003]). Attention increases neuronal activities responsible for the processing of the attended stimuli [Desimone and Duncan, 1995]. Most probably, endogenous attention facilitates the pathways that should be used by the attended stimuli [Egeth and Yantis, 1997]. In our model, facilitation can manifest itself through control action *within* cortical layers. On the other hand, awareness involves recurrent interactions between areas and can be suppressed by backward masking (see [Lamme, 2003] and references therein). This recurrent interaction required for awareness is our candidate function of the feedback connections between cortical areas.

Another note concerns top-down pattern completion: The controller network combines bottom-up information from different columns, areas and modalities and develops the *context* for lower level internal representation. Control action then corresponds to context based pattern completion. The efficiency of strong top-down control, such as overwriting, has been the subject of computer studies [Lőrincz et al., 2002b].

The merging of the two kinds of comparator networks solves the noise sensitivity of the controller. This noise filtering is fast and optimal, and it is an emerging property in the joined architecture.

According to the model, the EC deep layer to EC superficial layer synapses form the long-term memory of the EC-HC loop. On the other hand, the HC plays a particular, though not unique role. The HC is the top comparator that turns reconstruction error into control signal. This control signal excite the neurons of the EC deep layers. This is a unique position to encode inputs into the synapses between EC superficial and deep layers by Hebbian means. Similar roles can be played by all top-down control signals at other levels. These control signals target the deep layers and similarly to the HC output, they may enable (or facilitate) Hebbian learning of the LTM. Moreover, the control signal may

propagate from the higher reconstruction networks to lower ones and encoding at higher reconstruction networks may influence encoding at lower ones, too.

Our model, alike to its previous versions [Lőrincz, 1998, Lőrincz and Buzsáki, 2000, Lőrincz et al., 2002b] is neither a model for episodic learning, nor a model for incremental learning and does not fit such traditional distinctions (see, e.g., [Gluck et al., 2003]). On the one hand, when information maximization is not modulated by behavioral relevance, the model is an incremental model engaged in the maximization of information transfer, noise filtering and pattern completion using information theoretic algorithms in Hebbian forms [Lőrincz et al., 2002b]. On the other hand, the controller is a top-down tool, which can facilitate learning and could make learning instantaneous, if behavioral relevance requires: For a given input, and by activating a unit of the hidden layer, Hebbian learning will make that unit of the hidden layer to represent (encode) the actual input by means of its top-down synapses. Such mechanism can shortcut statistical analysis and may imprint the input into the internal representation. According to our model, the increased learning rate in deep layer afferents of the superficial layers corresponds to the supervisory instruction for the activated deep layer unit(s): Remember to the actual input!

The joined model offered no role for the recurrent collaterals of the superficial layers. We believe, that our continuous model can not uncover the role of these connectivity structures. Another missing feature of the neocortical structure is its columnar organization. The continuous comparator model does not seem to offer any clue here.

Finally, we note that the forming of invariant place cells from retinal input irrespective of the motion of eyes, head and body and their learned and optimized joined or disjoined motion patterns corresponds to a plant of very high order. Our rate code model justifies that invariant representations of place cells, the behaviorally important components of problem solving in mazes, are represented the hippocampus in rats and that the information of different modalities are associated here. (For a review, see, [Redish, 1999]).

## 5. CONCLUSIONS

There is a large body of experimental data supporting the idea that attention shapes (influences, controls) perception. For excellent reviews, see, e.g., [Duncan, 1999, Posner and DiGirolamo, 2000, LaBerge, 2000] and references therein. We have presented a unified model that optimizes bottom-up information transfer and filters (attenuates, prohibits) the propagation of structureless noise. The model also influences top-down processes, by comparing desired and experienced parameters in sensory information processing. The unification of the control model [Lőrincz, 1998] and the reconstruction architecture model [Lőrincz and Buzsáki, 2000] leads to falsifying predictions. Some of those predictions have gained experimental support recently. For example, the model predicts persistent activities in the deep layers of the entorhinal cortex that have been found in the experiments [Egorov et al., 2002]. Another falsifying prediction, that the circuitry of the dentate gyrus should support long delays, has also been reinforced [Henze et al., 2002]. A most intriguing prediction of the model is that the long-term memory of neocortical visual areas corresponds to the feedback connections between areas. These feedback connections are more numerous than the bottom-up connections between areas. However,

these feedback connections are relatively quiet. The model allowed us to distinguish between attention and awareness, two delicate and intertwined concepts. Known features of awareness allowed us to argue about the relative quietness of feedback connections between areas: there should be only one available representation for awareness, whereas multiple interpretations should coexist in representations not directly related to awareness. We have argued that this interpretation fits recent physiological findings.

#### ACKNOWLEDGEMENTS

This work was partially supported by Hungarian National Science Foundation (Grant No. OTKA T-32487). Special thanks are due to György Buzsáki for his enlightening and continuous support during the long-course of our model construction. Careful reading of the manuscript and helpful suggestions are gratefully acknowledged to György Hévízi and to Gábor Szirtes. I should thank the enlightening critical notes of Peter Dayan that have helped me in improving the presentation.

## REFERENCES

- [Amari, 1998] Amari, S. (1998). Natural gradient works efficiently in learning. *Neural Computation*, 10:251–276.
- [Amari et al., 1996] Amari, S., Cichocki, A., and Yang, H. (1996). A new learning algorithm for blind signal separation. In *Advances in Neural Information Processing Systems*, pages 757–763. Morgan Kaufmann, San Mateo, CA.
- [Bartels and Zeki, 2002] Bartels, A. and Zeki, S. (2002). The temporal limits of binding: Is binding post-conscious? In *Soc. Neurosci. Abstr.*, volume 11, page 260.
- [Bell and Sejnowski, 1995] Bell, A. J. and Sejnowski, T. J. (1995). An information-maximization approach to blind separation and blind deconvolution. *Neural Computation*, 7:1129–1159.
- [Callaway, 2000] Callaway, E. M. (2000). The mit encyclopedia of cognitive sciences. chapter Visual cortex, cell types and connections in, pages 867–869. MIT Press, Cambridge, MA.
- [Carpenter and Grossberg, 1987] Carpenter, G. and Grossberg, S. (1987). A massively parallel architecture for a self-organizing neural pattern recognition machine. *Computer Vision, Graphics and Image Processing*, 37:54–115.
- [Chrobak et al., 2000] Chrobak, J. J., Lőrincz, A., and Buzsáki, G. (2000). Physiological patterns in the hippocampo-entorhinal cortex system. *Hippocampus*, 10:457–465.
- [Comon, 1994] Comon, P. (1994). Independent component analysis - A new concept? *Signal Processing*, 36:287–314.
- [Desimone and Duncan, 1995] Desimone, J. and Duncan, J. (1995). Neural mechanisms of selective visual attention. *Annual Review of Neuroscience*, 18:193–222.
- [Diamond, 1979] Diamond, I. (1979). *Progress in Psychobiology and Physiological Psychology*, chapter The subdivision of neocortex: A proposal to revise the traditional view of sensory, motor and association areas, pages 1–43. Academic Press, New York.
- [Duncan, 1999] Duncan, J. (1999). *The MIT encyclopedia of cognitive sciences*, chapter Attention, pages 39–41. MIT Press, Cambridge, MA.
- [Egeth and Yantis, 1997] Egeth, H. and Yantis, S. (1997). Visual attention: Control, representation, and time course. *Annual Review of Psychology*, 48:269–297.
- [Egorov et al., 2002] Egorov, A. V., Hamam, B. N., Fransén, E., Hasselmo, M. E., and Alonso, A. A. (2002). Graded persistent activity in entorhinal cortex neurons. *Nature*, 420:173–178.
- [Eichenbaum, 2000] Eichenbaum, H. (2000). A cortical-hippocampal system for declarative memory. *Nature Reviews*, 1:41–50.
- [Gluck, 1996] Gluck, M. A. (1996). Computational models of hippocampal function in memory. *Hippocampus*, 6:565–762.
- [Gluck et al., 2003] Gluck, M. A., Meeter, M., and Myers, C. E. (2003). Computational models of the hippocampal region: linking incremental learning and episodic memory. *Trends in Cogn. Science*, 7. (in press).
- [Gluck and Myers, 1993] Gluck, M. A. and Myers, C. E. (1993). Hippocampal mediation of stimulus representation: A computational theory. *Hippocampus*, 3(4):491–516.
- [Grastyán et al., 1959] Grastyán, E., Lissák, K., Madarász, I., and Donhoffer, H. (1959). The hippocampal electrical activity during the development of conditioned reflexes. *Electroencephal. Clin. Neurophysiol.*, 11:409–430.
- [Grossberg, 1980] Grossberg, S. (1980). How does a brain build a cognitive code? *Psychol. Rev.*, 87:1–51.
- [Grossberg, 1982] Grossberg, S. (1982). Processing of expected and unexpected events during conditioning and attention: A psychophysiological theory. *Psychol. Rev.*, 89:529–572.
- [Grossberg and Carpenter, 1993] Grossberg, S. and Carpenter, G. A. (1993). Normal and amnesic learning, recognition, and memory by a neural model of cortico-hippocampal interactions. *Trends in Neurosciences*, 16:131–137.
- [Hasselmo and McClelland, 1999] Hasselmo, M. and McClelland, J. L. (1999). Neural models of memory. *Current Option in Neurobiology*, 9:184–188.

- [Hasselmo et al., 2002] Hasselmo, M. E., Bodelon, C., and Wyble, B. P. (2002). A proposed function for hippocampal theta rhythm: Separate phases of encoding and retrieval enhance reversal of prior learning. *Neural Comput.*, 14:793–817.
- [Hasselmo et al., 1996] Hasselmo, M. E., Wyble, B. P., and Wallenstein, G. V. (1996). Encoding and retrieval of episodic memories: Role of cholinergic and gabaergic modulation in the hippocampus. *Hippocampus*, 6:693–708.
- [Henze et al., 2002] Henze, D. A., Wittner, L., and Buzsáki, G. (2002). Single granule cells reliably discharge targets in the hippocampal ca3 network in vivo. *Nature Neurosci.*, 5:790–795.
- [Hwang and Ahuja, 1992] Hwang, Y. and Ahuja, N. (1992). Gross motion planning – a survey. *ACM Computing Surveys*, 24(3):219–291.
- [Hyvärinen, 1999] Hyvärinen, A. (1999). Sparse code shrinkage: Denoising of nongaussian data by maximum likelihood estimation. *Neural Computation*, 11:1739–1768.
- [Hyvärinen et al., 1999] Hyvärinen, A., Hoyer, P., and Oja, E. (1999). Sparse code shrinkage: Denoising by nonlinear maximum likelihood estimation. In *Advances in Neural Information Processing Systems 11 (NIPS\*98)*, pages 1739–1768. MIT Press.
- [Jutten and Herault, 1991] Jutten, C. and Herault, J. (1991). Blind separation of sources, Part I: An adaptive algorithm based on neuromimetic architecture. *Signal Processing*, 24:1–10.
- [Káli and Dayan, 2000] Káli, S. and Dayan, P. (2000). The involvement of recurrent connections in area ca3 in establishing the properties of place fields: A model. *J. Neurosci.*, 20:7463–7477.
- [Kalmár et al., 1998] Kalmár, Z., Szepesvári, C., and Lőrincz, A. (1998). Module-based reinforcement learning: Experiments with a real robot. *Machine Learning*, 31:55–85.
- [Karhunen et al., 1997] Karhunen, J., Oja, E., Wang, L., Vigarío, R., and Joutsensalo, J. (1997). A class of neural networks for independent component analysis. *IEEE Trans. on Neural Networks*, 8:487–504.
- [Kéri et al., 2002] Kéri, S., Janka, Z., Benedek, G., Aszalós, P., Szatmáry, B., Szirtes, G., and Lőrincz, A. (2002). Categories, prototypes and memory systems in Alzheimer’s disease. *Trends in Cognitive Sciences*, 6:132–136.
- [Knowlton, 1999] Knowlton, B. J. (1999). What can neuropsychology tell us about category learning? *Trends in Cog. Sci.*, 3:123–124.
- [Koch and Poggio, 1999] Koch, C. and Poggio, T. (1999). Predicting the visual world: Silence is golden. *Nature Neuroscience*, 2:9–10.
- [LaBerge, 2000] LaBerge, D. (2000). *The new cognitive neurosciences*, chapter Networks of attention, pages 711–724. MIT Press, Cambridge, MA, 2 edition.
- [Laheld and Cardoso, 1994] Laheld, B. and Cardoso, J. F. (1994). Adaptive source separation with uniform performance. In *Signal Processing VII: Theories and applications. Proceedings of EUSIPCO-94, Edinburgh, UK, September 1994*, volume 2, pages 183–186.
- [Lamme, 2003] Lamme, V. (2003). Why visual attention and awareness are different. *Trends in Cognitive Sciences*, 7:12–18.
- [Leopold, 2003] Leopold, D. A. (2003). Visual perception: Shaping what we see. *Current Biology*, 13:R10–R12.
- [Leopold and Logothetis, 1999] Leopold, D. A. and Logothetis, N. K. (1999). Multistable phenomena: Changing views in perception. *Trends in Cognitive Sciences*, 3:254–264.
- [Levy, 1996] Levy, W. B. (1996). A sequence predicting CA3 is a flexible associator that learns and uses context to solve hippocampal-like tasks. *Hippocampus*, 6:579–590.
- [Lisman, 1999] Lisman, J. E. (1999). Relating hippocampal circuitry to function: Recall of memory sequences by reciprocal dentate-ca3 interactions. *Neuron*, 22:233–242.
- [Lőrincz, 1998] Lőrincz, A. (1998). Forming independent components via temporal locking of reconstruction architectures: A functional model of the hippocampus. *Biological Cybernetics*, 79:263–275.
- [Lőrincz, 2003] Lőrincz, A. (2003). Controlled hierarchical filtering: Model of neocortical sensory processing. <http://www.arxiv.org/abs/cs.NE/0308025>.

- [Lőrincz and Buzsáki, 2000] Lőrincz, A. and Buzsáki, G. (2000). The parahippocampal region: Implications for neurological and psychiatric diseases. In Scharfman, H., Witter, M., and Schwarz, R., editors, *Annals of the New York Academy of Sciences*, volume 911, chapter Two-phase computational model training long-term memories in the entorhinal-hippocampal region, pages 83–111. New York Academy of Sciences, New York.
- [Lőrincz et al., 2001] Lőrincz, A., Hévízi, G., and Szepesvári, C. (2001). Ockham’s razor modeling of the matrix channels of the basal ganglia thalamocortical loop. *Int. J. of Neural Systems*, 11:125–143.
- [Lőrincz et al., 2002a] Lőrincz, A., Póczos, B., Szirtes, G., and Takács, B. (2002a). Ockham’s razor at work: Modeling of the ‘homunculus’. *Brain and Mind*, 3:187–220.
- [Lőrincz et al., 2002b] Lőrincz, A., Szatmáry, B., and Szirtes, G. (2002b). Mystery of structure and function of sensory processing areas of the neocortex: A resolution. *J. Comp. Neurosci.*, 13:187–205.
- [Lőrincz et al., 2002c] Lőrincz, A., Szirtes, G., Takács, B., Biederman, I., and Vogels, R. (2002c). Relating priming and repetition suppression. *Int. J. of Neural Systems*, 12:187–202.
- [Lőrincz et al., 2000] Lőrincz, A., Szirtes, G., and Takács, B. (2000). Is the hippocampus engaged in forming and encoding independent components of temporal sequences? In Bower, J., editor, *Conf. on Computational Neuroscience*. Elsevier.
- [Lund, 1988] Lund, J. S. (1988). Anatomical organization of macaque monkey striate visual cortex. *Annu. Rev. Neurosci.*, 11:253–288.
- [Mallat, 1998] Mallat, S. (1998). *A wavelet tour of signal processing*. Academic Press, San Diego, CA.
- [McClelland et al., 1995] McClelland, J. L., McNaughton, B. L., and O’Reilly, R. C. (1995). Why are there complementary learning systems in the hippocampus and neocortex. *Psychological Review*, 102:419–457.
- [Milner, 1972] Milner, B. (1972). Disorders of learning and memory after temporal lobe lesions in man. *Clin. Neurosurg.*, 19:421–446.
- [Myers et al., 1995] Myers, C. E., Gluck, M. A., and Granger, M. (1995). Dissociation of hippocampal and entorhinal function in associative learning: A computational approach. *Psychobiology*, 23:116–138.
- [O’Keefe and Nadel, 1978] O’Keefe, J. and Nadel, L. (1978). *The hippocampus as a cognitive map*. Oxford University Press, Oxford, UK.
- [Olshausen and Field, 1997] Olshausen, B. and Field, D. J. (1997). Sparse coding with an overcomplete basis set: A strategy employed by v1? *Vision Research*, 37:3311–3325.
- [O’Reilly and Rudy, 1999] O’Reilly, R. C. and Rudy, J. W. (1999). Conjunctive representations in learning and memory: Principles of cortical and hippocampal function. Technical report, Department of Psychology, University of Colorado, Boulder.
- [Otto and Eichenbaum, 1992] Otto, T. and Eichenbaum, H. (1992). Neuronal activity in the hippocampus during delayed non-match to sample performance in rats: Evidence for hippocampal processing in recognition memory. *Hippocampus*, 2:323–334.
- [Parker and Krug, 2003] Parker, A. and Krug, K. (2003). Neuronal mechanisms for the perception of ambiguous stimuli. *Current Opinion in Neurobiology*, 13:433–439.
- [Posner and DiGirolamo, 2000] Posner, M. I. and DiGirolamo, G. J. (2000). *The new cognitive neurosciences*, chapter Attention in cognitive neuroscience: An Overview, pages 623–631. MIT Press, Cambridge, MA, 2 edition.
- [Raizada and Grossberg, 2003] Raizada, R. and Grossberg, S. (2003). Towards a theory of the laminar architecture of cerebral cortex: Computational clues from the visual system. *Cerebral Cortex*, 13:100–113.
- [Ranck Jr., 1973] Ranck Jr., J. B. (1973). Studies on single neurons in dorsal hippocampal formation and septum in unrestrained rats. *Exp. Neurol.*, 41:461–555.
- [Rao, 1999] Rao, R. P. N. (1999). An optimal estimation approach to visual perception and learning. *Vision Research*, 39:1963–1989.
- [Rao and Ballard, 1997] Rao, R. P. N. and Ballard, D. H. (1997). Dynamic model of visual recognition predicts neural response properties in the visual cortex. *Neural Comput.*, 9:721–763.
- [Rao and Ballard, 1999] Rao, R. P. N. and Ballard, D. H. (1999). Predictive coding in the visual cortex: A functional interpretation of some extra-classical receptive-field effects. *Nature Neuroscience*, 2:79–87.

- [Redish, 1999] Redish, A. D. (1999). *Beyond the cognitive map: From place cells to episodic memory*. MIT Press, Cambridge, MA.
- [Rolls, 1989] Rolls, E. T. (1989). *Neural models of plasticity: Experimental and theoretical approaches*, chapter Functions of neuronal networks in the hippocampus and neocortex in memory, pages 240–265. Academic Press, San Diego. Eds.: J. H. Byrne and W. O. Berry.
- [Rolls, 2000] Rolls, E. T. (2000). Hippocampo-cortical and cortico-cortical backprojections. *Hippocampus*, 10:380–388.
- [Rolls et al., 1993] Rolls, E. T., Cahusac, P. M. B., Feigenbaum, J. D., and Miyashita, Y. (1993). Responses of single neurons in the hippocampus of the macaque related to recognition memory. *Exp. Brain. Res.*, 93:299–306.
- [Rugg, 1995] Rugg, M. D. (1995). *Handbook of Neuropsychology*, volume 10, chapter Cognitive event-related potentials: Intracranial and lesion studies, pages 165–185. Elsevier, New York.
- [Sidman et al., 1968] Sidman, M., Stoddard, L. T., and Mohr, J. P. (1968). Some additional quantitative observations of immediate memory in a patient with bilateral hippocampal lesions. *Neuropsychologia*, 6:245–254.
- [Sokolov, 1963] Sokolov, E. N. (1963). Higher nervous functions: the orienting reflex. *Annual Rev. Physiol.*, 25:545–580.
- [Squire, 1992] Squire, L. R. (1992). Memory and the hippocampus: A synthesis of findings with rats, monkeys, and humans. *Psychol. Rev.*, 99:195–231.
- [Szepesvári et al., 1997] Szepesvári, C., Cimmer, S., and Lőrincz, A. (1997). Neurocontroller using dynamic state feedback for compensatory control. *Neural Networks*, 10:1691–1708.
- [Szepesvári and Lőrincz, 1997a] Szepesvári, C. and Lőrincz, A. (1997a). *Applications of Neural Adaptive Control Technology*, chapter Approximate Inverse-Dynamics Based Robust Control Using Static and Dynamic Feedback, pages 151–179. World Scientific, Singapore.
- [Szepesvári and Lőrincz, 1997b] Szepesvári, C. and Lőrincz, A. (1997b). Robust control using inverse dynamics neurocontrollers. *Nonlinear Anal, Methods and Appl.*, 30:1669–1676.
- [Szepesvári and Lőrincz, 1998] Szepesvári, C. and Lőrincz, A. (1998). Integrated architecture for motion control and path planning. *J of Robotic Systems*, 15:1–15.
- [Szita and Lőrincz, 2003] Szita, I. and Lőrincz, A. (2003). Kalman filter control embedded into the reinforcement learning framework. *Neural Comp.* (in press).
- [Szita et al., 2003] Szita, I., Takács, B., and Lőrincz, A. (2003). Epsilon-MDPs: Learning in varying environments. *J. of Machine Learning Res.*, 3:145–174.
- [Vinogradova, 1975] Vinogradova, O. S. (1975). *The Hippocampus*, volume 2, chapter Functional organization of the limbic system in the process of registration of information: Facts and hypotheses, pages 3–69. Plenum Press, New York.
- [Wiebe and Saubli, 1999] Wiebe, S. P. and Saubli, U. V. (1999). Dynamic filtering of recognition memory codes in the hippocampus. *J. Neurosci.*, 19:10562–10574.
- [Zeki, 2003] Zeki, S. (2003). The disunity of consciousness. *Trends in Cognitive Science*, 7:214–218.